Dynamic CT Scanning for Visualization of the Parasellar Carotid Arteries

Wendy A. Cohen[1]
Richard S. Pinto
Irvin I. Kricheff

Evaluation of patients before transsphenoidal hypophysectomy for large intrasellar mass lesions has required bilateral internal carotid artery angiography. Using intravenous injection of contrast medium, a method has been developed to visualize the parasellar carotid arteries with rapid sequence sequential computed tomographic scanning. In 18 patients, the cavernous segments of the internal carotid arteries were well seen in 27 of 28 instances with technically complete examinations. The vascularity of the mass lesions and vascular encasement was also demonstrated.

The radiologic evaluation of abnormalities of the sella turcica before the development of computed tomography (CT) consisted of skull films, complex motion tomography, angiography, and pneumoencephalography. Enlargement of the sella turcica on plain films is most often caused by pituitary adenoma and is less commonly due to other lesions, such as craniopharyngioma, meningioma, dysgerminoma, teratoma, aneurysm, or an aberrant course of the internal carotid arteries [1]. A parasellar aneurysm may present with symptoms secondary to endocrinologic dysfunction or to local compression of the optic nerves, optic chiasm, or cavernous sinus without history of prior subarachnoid hemorrhage [2–4]. Widespread experience with CT has confirmed its value in both diagnosing and demonstrating the extension of an intrasellar or parasellar process [5]. However, identification of vascular abnormalities within the pituitary fossa and suprasellar cistern has remained difficult, and the differential diagnosis of a parasellar aneurysm versus tumor remains.

Many large intrasellar tumors are resected by a transsphenoidal approach. Before operation, bilateral internal carotid angiography has been performed to demonstrate the vascular anatomy, confirm tumor extension, show possible vascular encasement by tumor, and eliminate the possibility of a vascular lesion [6]. High-resolution CT after intravenous infusion of contrast material will adequately demonstrate the supraclinoid carotid arteries and allow differentiation of cavernous sinus from bone [7], but is unable to resolve the course of the carotid artery through the cavernous sinus.

We report a technique using rapid sequence scanning (dynamic CT) with variable interscan location and timing to visualize the parasellar vascular structures after an intravenous bolus injection of contrast medium. This has eliminated conventional angiography as a prerequisite for transsphenoidal surgery.

Materials and Methods

Eighteen patients were suspected of having abnormalities in the region of the sella turcica because of history, endocrine changes, visual changes, abnormalities on skull films, or demonstrated parasellar lesions on routine noncontrast and contrast enhanced CT. Dynamic CT was performed with a GE CT/T 8800 scanner using graphical data analysis capabilities available in experimental software and imaging programs supplied by General

This article appears in the March/April issue of *AJNR* and the May issue of *AJR*.

Received June 22, 1981; accepted after revision October 20, 1981.

Presented at the annual meeting of the American Society of Neuroradiology, Chicago, April 1981.

This work was supported in part by E. R. Squibb & Sons, Medical Developmental Department, Princeton, NJ 08540 and by General Electric, Milwaukee, WI 53201.

[1] All authors: Department of Radiology, New York University Medical Center, 550 First Ave., New York, NY 10016. Address reprint requests to W. A. Cohen.

***AJR* 138:905–909, May 1982**
0361–803X/82/1385–0905 $00.00
© American Roentgen Ray Society

Downloaded from www.ajronline.org by 2a01:4f9:3b:1ae9:: on 03/13/22 from IP address 2a01:4f9:3b:1ae9::. Copyright ARRS. For personal use only; all rights reserved

Downloaded from www.ajronline.org by 2a01:4f9:3b:1ae9:: on 03/13/22 from IP address 2a01:4f9:3b:1ae9::. Copyright ARRS. For personal use only; all rights reserved

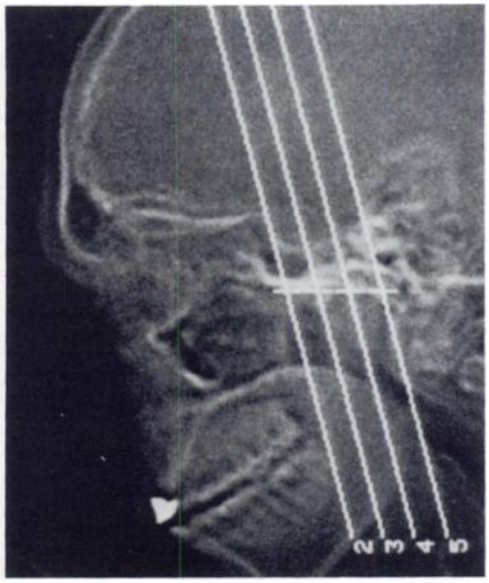

Fig. 1.—Lateral skull "scout view" showing scan positioning for coronal dynamic CT. Lines mark levels of scans. Line 2 is first scan as described in part 1 of Materials and Methods.

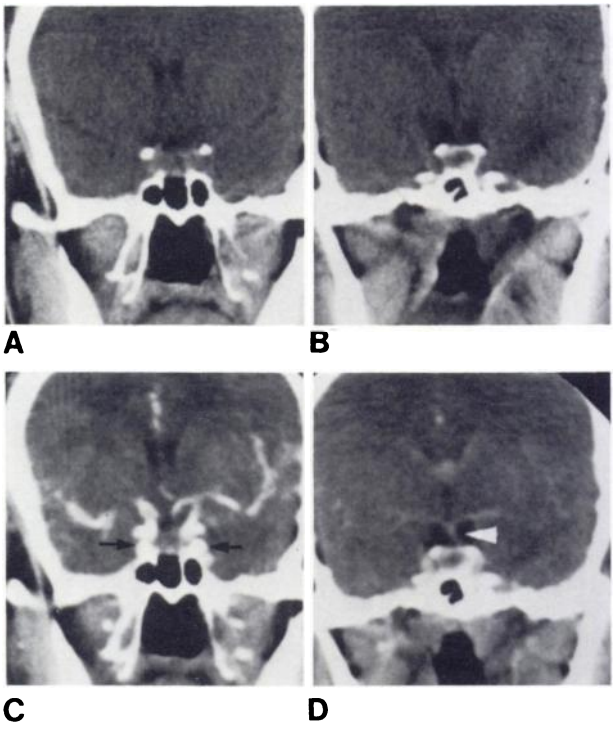

Fig. 2.—Normal coronal dynamic CT scans. **A** and **B**, Preliminary scans of sella turcica and dorsum. **C** and **D**, After bolus contrast injection. Parasellar carotid arteries (*black arrows*), supraclinoid vessels, and basilar artery (*white arrowhead*).

Electric (GEDIS 6.16–6.21). The examination consisted of two parts with an optional third part.

For each part, baseline scans through the structures of interest were performed. Initial levels were chosen from a digitized image of the lateral head ("scout view"). The images were obtained with or without contrast enhancement. For the dynamic study an intravenous bolus injection of Renografin-76 was given through an 18 gauge angiocatheter in a large antecubital vein. All injections were with a mechanical injector, delivering 40 ml of warmed contrast agent (11 g iodine) over 4–5 sec.

Arm to brain transit time in adults, determined empirically, is about 8 sec. The scanner required 2 sec for rotor preparation, thus the injection was started 4 sec before the commencement of the initial scan. Maximum contrast density appeared in vascular structures in the second and third scans of a rapid sequence series.

Using the rapid sequence scanning method, a single scan was obtained over 4.8 sec. Using the table increment mode, 6.5 sec. were required between scans, during which time the table changed locations to a preprogrammed position. If the scan location was not changed, interscan time could be reduced to 1.5 sec.

Part 1 (Coronal Scanning)

The patient was placed in a position for direct coronal scanning, lying prone with his head extended and the scanner gantry tilted so that the scan plane was approximately perpendicular to the planum sphenoidale. Gantry angulation and scan position were determined from the "lateral" scan view. Baseline 10-mm-thick adjacent noncontrast scans were obtained, starting 10 mm in front of the tips of the anterior clinoids to encompass a part of the planum sphenoidale and tuberculum, and ending behind the dorsum sellae (fig. 1).

The routine dynamic CT series consisted of four to five scans taken at the same locations as the baseline scans using the table increment mode and a bolus injection of contrast agent. Scanning started at the most anterior point of the baseline scans and moved posteriorly. Baseline and dynamic CT scans were compared to differentiate vascular structures from bone, cavernous sinus, or tumor (fig. 2).

Part 2

The patient was repositioned supine, and adjacent 10-mm-thick baseline scans were obtained starting 10 mm inferior to the floor of the sella and ending at the level of the suprasellar cistern. Dynamic CT scans were again obtained, combined with a bolus intravenous injection of contrast material at the same levels as the baseline scans. The second scan (which has maximum change in contrast density) included the anterior clinoids. Scanning started at the more caudal level and moved craniad.

Part 3 (Optional)

If a question remained concerning the vascularity of a visualized structure, rapid sequence imaging, combined with an intravenous bolus injection of contrast medium, was performed through the midpart of the structures to be identified in a single location. For these patients, graphic analysis of change in contrast density over time within specific structures was performed. After a representative area within a structure was chosen, computer programs were available that averaged the CT number within the region for each scan of the dynamic CT series. The data were presented with either absolute CT number or the change in CT number (Δ Hounsfield units [H]) plotted as a function of scan time.

Downloaded from www.ajronline.org by 2a01:4f9:3b:1ae9:: on 03/13/22 from IP address 2a01:4f9:3b:1ae9::. Copyright ARRS. For personal use only; all rights reserved

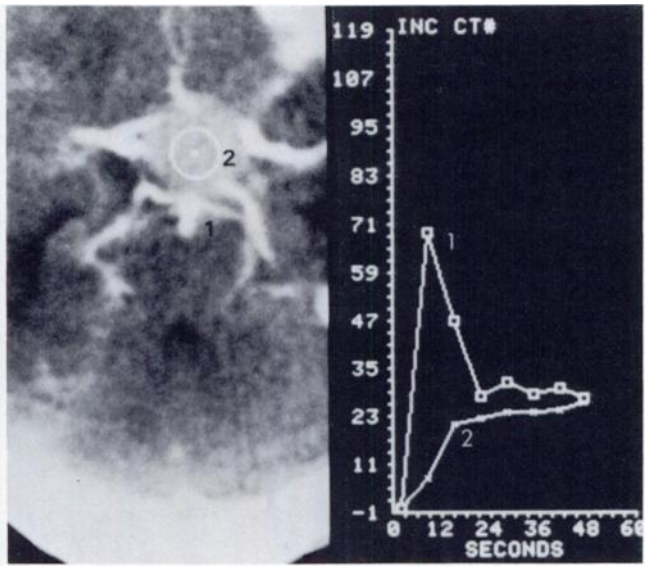

Fig. 3.—Dynamic CT scan, axial plane. Vessels of circle of Willis in patient with pituitary adenoma. Regions of interest centered on basilar artery (1) and pituitary adenoma (2). Graphs show change of CT number with time (Δ Hounsfield units). Graph 1, normal vascular pattern. Graph 2, slower rise to plateau found with many adenomas.

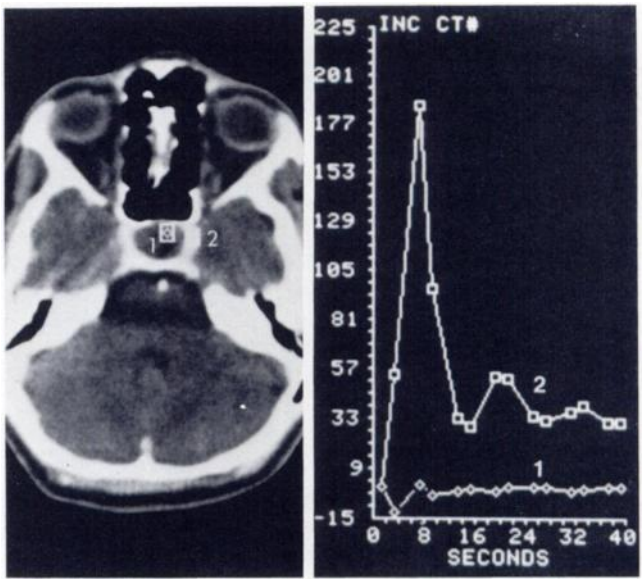

Fig. 4.—Dynamic CT scan of craniopharyngioma. Regions of interest centered over sella turcica (1) and intracavernous carotid artery (2). Graphs of increased CT number (INC CT#). Graph 1, pattern of craniopharyngioma, little appreciable change in contrast density. Graph 2, pattern of vascular structures.

Results

Pathologic entities in the 18 patients consisted of pituitary adenoma (11 patients), pituitary microadenoma (2), craniopharyngioma (2), microadenoma after radiotherapy (1), and normal pituitary (2). Another patient with a sphenoid wing meningioma is included in this report. This patient had a dynamic CT scan of the lesion (as in part 3); however, no attempt was made to visualize the other parasellar vessels.

Six patients had incomplete studies: three initial patients had only one part of our protocol performed and three had early termination of the study due to extravasation of contrast agent into the soft tissues of the upper arm. Eight patients were also studied angiographically. Fourteen patients were studied as per protocol and form the basis of this analysis.

The cavernous segment of the right internal carotid artery was well visualized in 13 (93%) of 14 patients but only partially seen in 1 (7%) of 14. The cavernous segment of the left internal carotid artery was well seen in all patients. Both supraclinoid carotid arteries were demonstrated in 10 (71%) of 14 and one of the two arteries was seen in 1 (7%) of 14. The A1 segment of the anterior cerebral artery was seen in 10 (71%) of 14.

The maximal attenuation values of both arterial structures and of various lesions were assessed. The parasellar carotid arteries on axial projections ranged from 94 to 258 H (mean, 170 H) and on coronal projections from 123 to 448 H (mean, 237 H). Adenomas on either axial or coronal scans ranged from 41 to 105 H (mean, 65 H). If a change in CT number (ΔH) alone is considered, carotid arteries on axial scans ranged from 89 to 170 H (mean, 120 H); on coronal scans, 44 to 185 H (mean, 94 H); and pituitary adenoma, 2 to 27 H (mean, 17 H). The single meningioma studied had a maximum attenuation value of 75 H and a ΔH of 41 H. Craniopharyngiomas did not significantly change in density.

Graphical Analysis

Contrast density change (ΔH) was plotted against time for the 14 patients who had dynamic scans performed in a single plane (fig. 3). Plots obtained from arterial structures demonstrated a rapid, sharp rise and fall in attenuation values over the first 15–20 sec. A second, small recirculation curve occurred during the next 15–20 sec, which was 26–40 sec from the initial scan. For these vascular structures the baseline absolute CT density was in the range of 60–80 H after the first injection of contrast material. ΔH varied from 70 to 180 H, and after the early large peak, a plateau ranging between 14 and 41 H (mean, 25 H) occurred. Similar analysis of the appearance of contrast material in pituitary adenomas demonstrated a gradual increase in attenuation value during the first 30 sec after the intravenous bolus injection of contrast material. Subsequently, the curve formed a plateau ranging between 6 and 25 H (mean, 12 H) that extended into the recirculation phase. The slope of the initial wash-in phase for pituitary adenomas was flatter than that obtained from vascular structures. Even tumors that had early peaks in contrast density in a time similar to that of arterial structures demonstrated a slow rise after the initial "arterial" phase and arterial peaks, which were lower in maximum CT number than those seen in vascular structures. The least contrast passage occurred in craniopharyngiomas, which demonstrated insignificant early changes in CT attenuation values and little enhancement at any time (fig. 4). In all cases, it was possible to differentiate a primary vascular structure from a soft-tissue structure.

Downloaded from www.ajronline.org by 2a01:4f9:3b:1ae9:: on 03/13/22 from IP address 2a01:4f9:3b:1ae9::. Copyright ARRS. For personal use only; all rights reserved

Discussion

Angiography of both internal carotid arteries in patients with large sellar and parasellar lesions continues to be used to localize vascular structures, to demonstrate displacements, and to rule out a vascular etiology of the intrasellar pathology. Conventional CT clearly shows the supraclinoid carotid arteries; however, the rapid, early enhancement of pituitary adenomas may preclude separation of tumor from the enhanced cavernous sinus and parasellar carotid arteries. Arteriography of the carotid arteries clearly demonstrates suprasellar tumor extension by elevation of the A1 segments of the anterior cerebral arteries, but the lateral extent of the tumor can only be described if there is spread outside the sella turcica that either displaces or visibly encases the cavernous segment of the internal carotid artery [8, 9]. In some cases, encasement can only be inferred from a combination of CT and angiographic findings. In one of our cases, dynamic CT was able to demonstrate the carotid artery embedded within a tumor that extended laterally beyond the vessel, a finding not appreciated angiographically (fig. 5).

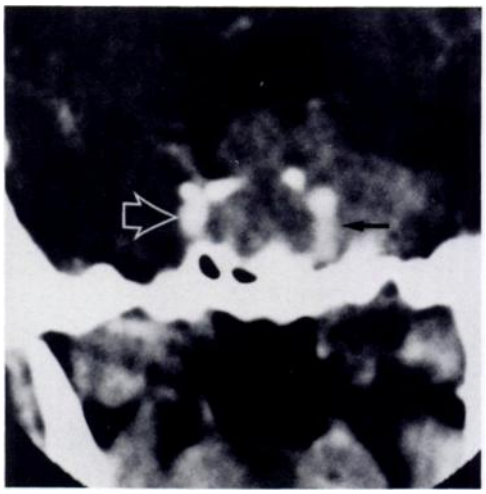

Fig. 5.—Dynamic CT scan of recurrent pituitary adenoma. Encasement of right carotid artery by lateral tumor extension. Right (*black arrow*) and left (*open arrow*) intracavernous carotid arteries.

A previous report of dynamic CT [10] characterized the change in contrast density in relation to time of various lesions after bolus injection of contrast material. Vascular lesions had a large change in contrast density with steep, early rising and down slopes, while pituitary adenomas demonstrated a slow rise, broad peaks, and a gradual decrease in contrast density with a maximum peak at 2 min (fig. 3). Even during the second and third parts of our protocol, when patients had already received contrast material, the higher peak and marked change of density of vascular structures allowed the differentiation of vessels from intrasellar mass lesions with prior contrast enhancement. Nonvascular structures were also clearly distinguished. Due to the intensity of the contrast enhancement in vascular structures, in most cases it was unnecessary to compare dynamic CT with baseline CT scans to distinguish vascular structures from bone in the region of the sella.

In a patient with an enlarged pituitary fossa, accurate identification of the location of the parasellar vessels on a single noncontrast scan is difficult. To assure that no vascular abnormality is present, the carotid artery within the cavernous sinus as well as in the supraclinoid region must be visualized, which requires a rapid change of scan position. For most patients with enlargement of the sella, its entire volume can be imaged in two 10 mm scans. Using a 5 sec injection rate and the table increment mode, parasellar vascular structures could be visualized on the two scans that encompassed the sella (fig. 6). If an abnormal vascular structure in a parasellar or intrasellar location continued to be suspected, a dynamic CT scan centered over the suspected lesion was obtained. This scan sequence constituted the optional third part of our protocol. Another use of the optional third part was to provide further information about the vascular anatomy around the circle of Willis. In two cases, this provided a better definition of the supraclinoid vessels, particularly the A1 segments of the anterior cerebral arteries. However, the primary use of the third part was to obtain transit time analyses.

For most patients it was necessary to obtain both axial and coronal scans, although if parasellar vascular structures could be clearly identified after a single injection, one series would be adequate. For example, in two cases, one cavernous carotid artery segment was not well seen on coronal scans but was visualized in its intracavernous position on axial dynamic CT. During the initial phases of our study, we performed two injections to confirm the validity of the method.

A difficulty in imaging parasellar vascular structures on dynamic CT occurred if the intrasellar mass lesion was large and markedly displaced the carotid arteries. The internal carotid arteries in a patient with a large craniopharyngioma were poorly seen, although the absence of vascular structures within the sella was clearly demonstrated. A second patient, as yet not operated upon, has marked lateral extension of tumor. The laterally displaced vessel was visualized but its course through the cavernous region was poorly resolved.

Cerebral angiography by the femoral route has been reported to have a risk of major complications of 0.28% and of minor complications of 6.65% [11]. Dynamic CT has a risk of a major complication the same as that of any intravenous injection of contrast material. The minor complications—extravasation of contrast material into the upper arm—resulted in local discomfort for 15 to 30 min, easily relieved by warm soaks. No permanent sequela occurred. These complications occurred early in our investigation when injection rates of greater than 10 ml/sec were used. At our current injection rate of 8 ml/sec, no contrast medium extravasation has occurred. The multiple injections of contrast material delivered a maximum total iodine dose of 44.4 g if all three parts of the protocol were used. Fluids were encouraged after the examination. All patients had normal renal function and no renal complications.

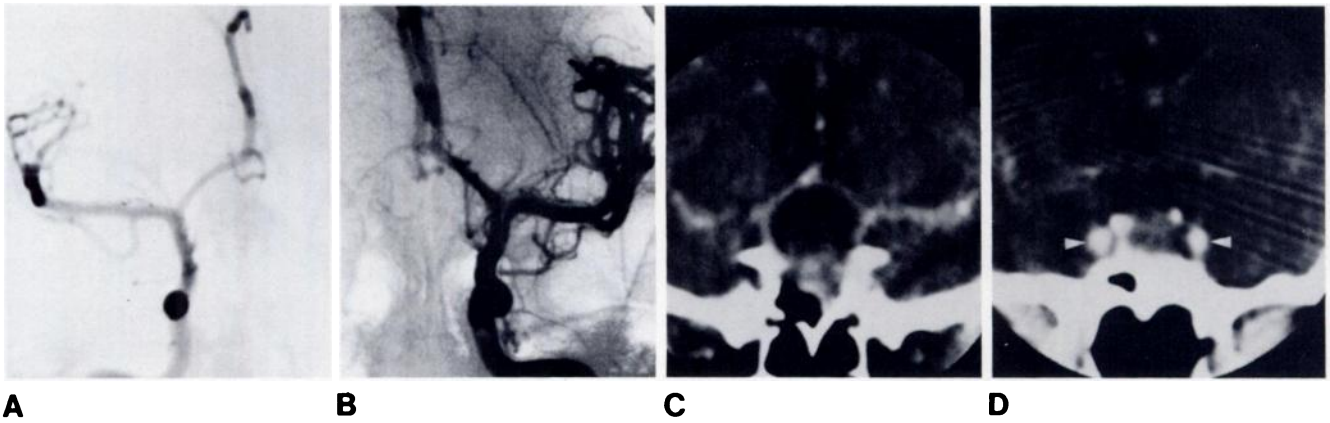

Fig. 6.—Craniopharyngioma. **A** and **B**, Internal carotid artery injections showing upward displacement of A1 segment of anterior cerebral arteries. **C** and **D**, Coronal dynamic CT scan of same patient, similar vascular configuration. **C**, Elevated A1 segments. **D**, Cavernous carotid arteries (*arrowheads*).

Our study proved that rapid sequence CT imaging in our protocol will visualize well the parasellar vascular tree, locate major vessels encased by tumor, and eliminate the possibility of a vascular lesion in the differential diagnosis of a parasellar tumor. Since it requires only intravenous injection of contrast material, it may be performed on an outpatient basis. Dynamic CT is, in our opinion, a viable alternative to angiography as a prerequisite to transsphenoidal surgery of parasellar tumors.

ACKNOWLEDGMENTS

We thank Patricia Lewis for technical assistance and Lydia Logozo, Linda Michaels and Jill Tepper for assistance in manuscript preparation.

REFERENCES

1. Boyce DW, Huckman MS. Contiguous internal carotid arteries in empty sella syndrome. *Radiology* **1976**;120:120
2. White JC. Aneurysms mistaken for hypophyseal tumors. *Clin Neurosurg* **1964**;10:224–250
3. Bull JWD. Contribution of radiology to the study of intracranial aneurysms. *Br Med J* **1962**;2:1701–1708
4. Heisakanen O, Nikki P. Large intracranial aneurysms. *Acta Neurol Scand* **1962**;38:195–208
5. Naidich TP, Pinto RS, Kushner MJ, Lin JP, Kricheff II, Leeds NE, Chase NE. Evaluation of sella and parasellar masses by computer tomography. *Radiology* **1976**;120:91–99
6. Kern EB, Pearson BW, McDonald TJ, Laws ER Jr. The transseptal approach to lesions of the pituitary and parasellar regions. *Laryngoscope* **1979**;89:1–34
7. Hayman LA, Evans RA, Hinck VC. Rapid high dose (RHD) contrast computed tomography of parisellar vessels. *Radiology* **1979**;131:121–123
8. Taveras JM, Wood EH. *Diagnostic neuroradiology*. Baltimore: Williams & Wilkins, **1976**:737–738
9. Epstein BS, Epstein JA. The angiographic demonstration and surgical implications of imbedding of the carotid syphons by a large pituitary adenoma. *AJR* **1968**;104:162–167
10. Wing SD, Anderson RE, Osborn AG. Dynamic cranial computed tomography: preliminary results. *AJNR* **1980**;1:135–139
11. Huckman MS, Shenk GL, Neems RL, Tinor T. Transfemoral cerebral arteriography versus direct percutaneous carotid and brachial arteriography: a comparison of complication rates. *Radiology* **1979**;132:93–98

Downloaded from www.ajronline.org by 2a01:4f9:3b:1ae9:: on 03/13/22 from IP address 2a01:4f9:3b:1ae9::. Copyright ARRS. For personal use only; all rights reserved